

# New Results on Diffractive $t$ -Distributions from CDF

Konstantin Goulianos\*

The Rockefeller University, 1230 York Avenue, New York, NY 10065, USA

DOI: will be assigned

We present a measurement of antiproton ( $\bar{p}$ ) four-momentum transfer distributions,  $t_{\bar{p}}$ , for inclusive and dijet single-diffractive production at  $\sqrt{s}=1.96$  TeV at the Fermilab Tevatron  $\bar{p}p$  Collider. We use data collected by the CDF II detector equipped with a Roman Pot Spectrometer that measures  $t_{\bar{p}}$  and the  $\bar{p}$  forward momentum loss,  $\xi_{\bar{p}}$ . We report results for  $0.05 < \xi_{\bar{p}} < 0.08$ ,  $-t_{\bar{p}} \leq 4$  GeV<sup>2</sup>, and jet transverse energies,  $E_T^{\text{jct}}$ , of  $10^2 < Q^2 \approx (E_T^{\text{jct}})^2 < 10^4$  GeV<sup>2</sup>. In addition, we search for diffractive dips in both the inclusive and dijet distributions, and compare all results with theoretical expectations.

## 1 Introduction

We present a measurement of four-momentum-transfer ( $t$ ) distributions for inclusive and dijet single-diffractive (SD) production in  $\bar{p}p$  collisions at  $\sqrt{s} = 1.96$  TeV,  $\bar{p}+p \rightarrow \bar{p}+G_{\bar{p}}+X_p$ , where  $G_{\bar{p}}$  is a region of pseudorapidity<sup>1</sup> devoid of particles (rapidity gap), and  $X$  represents particles from the dissociation of the proton [1]. The rapidity gap, presumed to be caused by a color-singlet exchange with vacuum quantum numbers between the  $\bar{p}$  and the dissociated proton, traditionally referred to as Pomeron ( $\mathbb{P}$ ) exchange, is related to  $\xi_{\bar{p}}$ , the forward momentum loss of the surviving  $\bar{p}$ , by  $G_{\bar{p}} = -\ln \xi_{\bar{p}}$ . Using data collected by the CDF II detector, equipped with a Roman Pot Spectrometer (RPS) that measures  $t_{\bar{p}}$  and  $\xi_{\bar{p}}$  for each event, we extract  $t_{\bar{p}}$  distributions for events within  $0.05 < \xi_{\bar{p}} < 0.08$ . We cover the ranges of  $-t_{\bar{p}} \leq 4$  GeV<sup>2</sup> and jet transverse energy,  $E_T^{\text{jct}}$ , of  $10^2 < Q^2 \approx (E_T^{\text{jct}})^2 < 10^4$  GeV<sup>2</sup>, search for diffractive dips, and compare all results with theoretical expectations.

## 2 Measurement

**Detector.** Figure 1 is a schematic plan view of the detector used in this measurement, showing the main detector (CDF II) and the forward detector-components used in the diffractive-physics measurements. The forward detectors include a Roman Pot Spectrometer (RPS), which measures  $\xi_{\bar{p}}$  and  $t_{\bar{p}}$  with resolutions  $\delta\xi_{\bar{p}} = 0.001$  and  $\delta t_{\bar{p}} = \pm 0.07$  GeV<sup>2</sup> at  $\langle -t_{\bar{p}} \rangle \approx 0.05$  GeV<sup>2</sup>, where  $\delta t_{\bar{p}}$  increases with  $t_{\bar{p}}$  with a  $\propto \sqrt{-t_{\bar{p}}}$  dependence.

\*Presented on behalf of the CDF Collaboration.

<sup>1</sup>Rapidity,  $y = \frac{1}{2} \ln \frac{E+p_L}{E-p_L}$ , and pseudorapidity,  $\eta = -\ln \tan \frac{\theta}{2}$ , where  $\theta$  is the polar angle of a particle with respect to the proton beam ( $+\hat{z}$  direction), are used interchangeably for particles detected in the calorimeters, since in the kinematic range of interest in this analysis they are approximately equal.

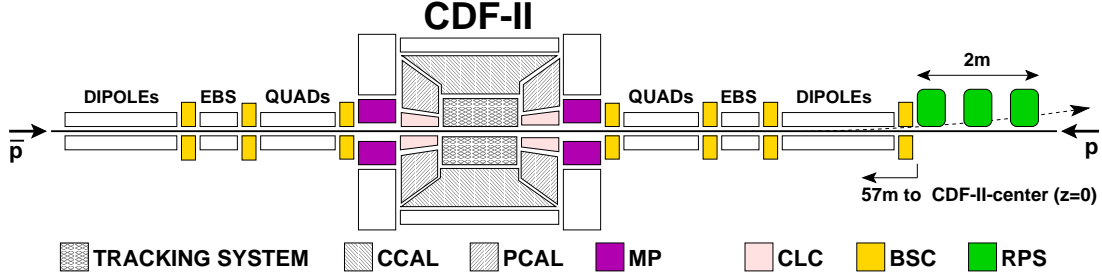


Figure 1: Schematic plan view of the detector, showing the main detector (CDF II) with the tracking system and calorimeters (central, CCAL; plug, PCAL), and the forward components (Cerenkov Luminosity Counters, CLC; MiniPlugs, MP; Roman Pot Spectrometer, RPS). The beamline elements labeled EBS are the electrostatic beam separators.

**Data samples.** This analysis is based on data corresponding to an integrated luminosity  $\mathcal{L} \approx 310 \text{ pb}^{-1}$  collected in 2002–2003. Events are selected online with a three-level prescaled triggering system, which accepts RPS-triggered inclusive events, as well as jet-enriched events, by requiring at least one calorimeter tower with  $E_T > 5, 20, \text{ or } 50 \text{ GeV}$  within  $|\eta| < 3.5$ . Jets are reconstructed using the midpoint algorithm [2].

The following trigger definitions are used for measuring  $t_{\bar{p}}$  distributions:

- RPS: requires the RPS trigger counters to be in time with a  $\bar{p}$  crossing the CDF II nominal interaction region;
- J5 (J20, J50): jet with  $E_T^{\text{jet}} \geq 5 \text{ (20, 50) GeV}$  in CCAL or PCAL;
- RPS·Jet5 (Jet20, Jet50): RPS trigger in coincidence with J5 (J20, J50).

**RPS alignment.** The measurements of  $t_{\bar{p}}$  require precise alignment of the RPS detectors relative to the actual position of the beam at the time of data collection. We developed a *dynamic alignment* method that is applied offline to the collected data samples. The method consists of introducing offsets in the nominal  $x$  and  $y$  coordinates of the RPS detectors relative to the beam, fitting data for  $-t \leq 1 \text{ GeV}^2$  with a form composed of two exponential terms,

$$\frac{dN_{\text{events}}}{dt} = N_{\text{norm}} (A_1 e^{b_1 t} + A_2 e^{b_2 t}), \quad (1)$$

where  $N_{\text{norm}}$  is a normalization factor, and iteratively adjusting the offsets until a maximum for  $dN_{\text{events}}/dt$  at  $t_{\bar{p}} = 0$  is obtained. To improve the fits, we set  $A_2/A_1 = 0.11$ , which is the average value over all data subsamples, and repeat the iterative fitting. This method yields an accuracy of  $\pm 60 \mu\text{m}$  in the beam position, which leads to a systematic uncertainty of  $\pm 5\%$  in  $b_1$  and  $b_2$ .

### 3 Results

**$t_{\bar{p}}$  distributions for  $-t_{\bar{p}} \leq 1 \text{ GeV}^2$ .** Inclusive and jet-enriched data of  $10^2 < Q^2 \approx (E_T^{\text{jet}})^2 < 10^4 \text{ GeV}^2$  have been studied. Results for  $t_{\bar{p}}$ -distribution shapes are shown in Fig. 2

and in table 1. No significant  $Q^2$  dependence is observed from  $\langle Q^2 \rangle \approx 1 \text{ GeV}^2$  (inclusive) to  $Q^2 \approx 10^4 \text{ GeV}^2$ . The mean values of  $b_1$  and  $b_2$  over all the data samples are  $5.27 \pm 0.33 \text{ GeV}^{-2}$  and  $1.17 \pm 0.17 \text{ GeV}^{-2}$ , respectively. Systematic uncertainties in  $b_1$  and  $b_2$  are due to RPS-tracker thresholds(1%), instantaneous luminosity (2%), beam conditions (4%), and RPS alignment (5%). These uncertainties are correlated among all data points, and when added in quadrature yield an overall total uncertainty of  $\delta b_{1,2}^{\text{sys}} = \pm 9.7\%$ . The measured slopes of the inclusive sample are in agreement with expectations from the Donnachie-Landshoff (DL) model [3]. The  $Q^2$  near-independence of the  $t_{\bar{p}}$  distributions favors models of hard-diffractive production in which the hard scattering is controlled by the parton distribution function of the recoil antiproton, while the rapidity-gap formation is governed by a color-neutral soft exchange [4]-[7].

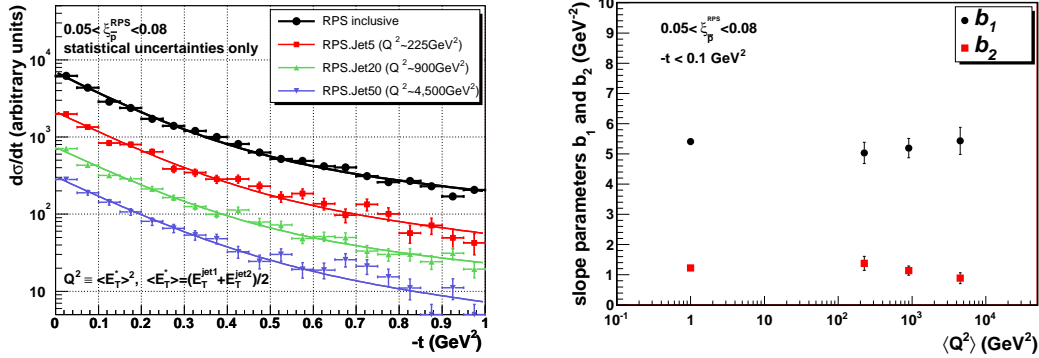


Figure 2: (left)  $t_{\bar{p}}$  distributions for SD RPS data of various average  $Q^2$  values within  $0.05 < \xi_{\bar{p}}^{\text{RPS}} < 0.08$ ; (right) the slope parameters  $b_1$  and  $b_2$  vs  $\langle Q^2 \rangle$  of a fit to the form  $dN_{\text{events}}/dt = N_{\text{norm}}(A_1 e^{b_1 t} + A_2 e^{b_2 t})$ , with  $A_2/A_1 = 0.11$  (average over all data subsamples). The RPS inclusive points have been placed arbitrarily at  $\langle Q^2 \rangle = 1 \text{ GeV}^2$ .

Table 1: Slopes of  $t_{\bar{p}}$  distributions of SD RPS data within  $0.05 < \xi_{\bar{p}}^{\text{RPS}} < 0.08$  for inclusive and dijet event samples of various  $\langle E_T^* \rangle$  or  $Q^2 \equiv \langle E_T^* \rangle^2$  values obtained from fits to the form  $dN_{\text{events}}/dt = N_{\text{norm}}(A_1 e^{b_1 t} + A_2 e^{b_2 t})$  with  $A_2/A_1 = 0.11$ , fixed at the average value obtained in the dynamic alignment of all different event subsamples. The uncertainties listed are statistical.

Event sample	$\langle E_T^* \rangle$ (GeV)	$Q^2$ (GeV <sup>2</sup> )	$b_1$ (GeV <sup>-2</sup> )	$b_2$ (GeV <sup>-2</sup> )	$b_1/b_1^{\text{incl}}$	$b_2/b_2^{\text{incl}}$
RPS	incl	$\approx 1$	$5.4 \pm 0.1$	$1.2 \pm 0.1$	1	1
RPS·Jet5	15	225	$5.0 \pm 0.3$	$1.4 \pm 0.2$	$0.93 \pm 0.08$	$1.12 \pm 0.23$
RPS·Jet20	30	900	$5.2 \pm 0.3$	$1.1 \pm 0.1$	$0.96 \pm 0.07$	$0.93 \pm 0.16$
RPS·Jet50	67	4500	$5.5 \pm 0.5$	$0.9 \pm 0.2$	$1.00 \pm 0.10$	$0.72 \pm 0.18$

$t_{\bar{p}}$  distributions for  $-t_{\bar{p}} \leq 4 \text{ GeV}^2$  and search for diffractive dips. Figure 3 (left) shows  $t_{\bar{p}}$  distributions in the region of  $-t_{\bar{p}} \leq 4 \text{ GeV}^2$  for the inclusive and the RPS-jet20 data

of  $\langle Q^2 \rangle \simeq 900 \text{ GeV}^2$ . The following prominent features are observed: (i) the two distributions are similar in shape, (ii) the inclusive distribution follows the DL prediction for  $-t_{\bar{p}} \lesssim 0.5 \text{ GeV}^2$ , but lies increasingly higher than the DL curve as  $-t_{\bar{p}}$  increases, becoming approximately flat for  $-t_{\bar{p}} \gtrsim 2 \text{ GeV}^2$ . As the  $t_{\bar{p}}$  acceptance, shown in Fig. 3 (*right*), varies slowly in this region, and the overall  $t_{\bar{p}}$  resolution at  $-t_{\bar{p}} \approx 2.5 \text{ GeV}^2$  is  $\approx \pm 1 \text{ GeV}^2$ , we conclude that the observed flattening-out of the distributions is physics-based, possibly caused by an underlying diffractive dip at  $t_{\bar{p}} \approx 2.5 \text{ GeV}^2$  filled-out by resolution effects.

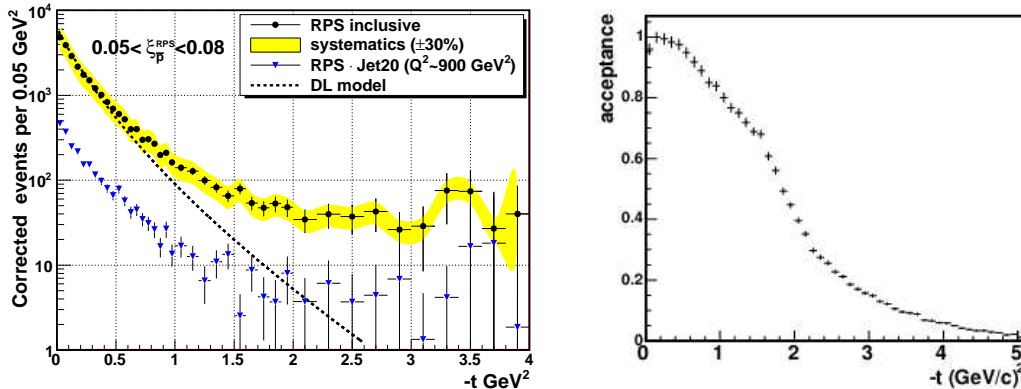


Figure 3: (*left*)  $t$  distributions of two data samples of SD RPS events within  $0.05 < \xi_{\bar{p}}^{\text{RPS}} < 0.08$  corrected for RPS acceptance after background subtraction: RPS inclusive,  $\langle Q^2 \rangle \simeq 1 \text{ GeV}^2$  (circles), and RPS-Jet20,  $\langle Q^2 \rangle \simeq 900 \text{ GeV}^2$  (triangles); the curve is the expectation of the DL model normalized to the RPS inclusive data within  $-t \lesssim 0.5 \text{ GeV}^2$ . (*right*) RPS acceptance vs  $-t_{\bar{p}}$ , integrated over the region of  $0.05 < \xi_{\bar{p}} < 0.08$ .

## 4 Acknowledgments

I would like to thank Michele Gallinaro, Koji Terashi, Mary Convery, and Christina Mesropian for invaluable contributions to this analysis, my colleagues at the CDF Collaboration, and the Office of Science of the Department of Energy for its generous financial support.

## References

- [1] V. Barone and E. Predazzi, “High-Energy Particle Diffraction”, Springer Press, Berlin, (2002).
- [2] G. C. Blazey *et al.*, “Run II Jet Physics”, in *Proceedings of the Run II QCD and Weak Boson Physics Workshop*. arXiv:hep-ex/0005012, 2000.
- [3] A. Donnachie and P. Landshoff, Phys. Lett. **B518** (2001) 63.
- [4] K. Goulianos, “Renormalized Diffractive Parton Densities,” in *Diffraction 06, International Workshop on Diffraction in High-Energy Physics*, Adamantas, Milos island, Greece (2006). PoS (DIFF2006) 044.
- [5] S. J. Brodsky *et al.*, Phys. Rev. D **71** (2005) 074020.
- [6] A. B. Kaidalov *et al.*, Eur. Phys. J. C **21** (2001) 521. Eur. Phys. J. C **21** (2001) 521.
- [7] B. Z. Kopeliovic *et al.*, Phys. Rev. D **76**, 034019 (2007).